STUDY AND DESIGN OF A FAST SWITCHING MAGNET FOR THE MYRRHA PROJECT*

E. Froidefond[†], F. Bouly, P.-O. Dumont, LPSC, Grenoble, France
D. Vandeplassche, SCK, CEN, Louvain-la-Neuve, Belgium

Abstract

The MYRRHA project aims at building an Accelerator Driven System demonstrator, which consists of two injectors, a superconducting linac (SC) and a sub-critical nuclear reactor. The Medium Energy Beam Transport line (MEBT) brings the proton beam of the first injector, accelerated up to 17 MeV to the linac (600 MeV). In the meantime, the beam from the second injector is sent to a beam dump. In case of a failure of the first injector, the awaiting beam of the second injector is deviated to the linac. A switching magnet located at the junction of the two injection lines performs this beam switch in less than 1.5 seconds. A magnetic design and a mechanical structure of this magnet proposed to the MYRRHA project are presented.

THE MYRRHA ACCELERATOR

Overview of the Project

The MYRRHA (Multi-purpose hYrid Research Reactor for High-tech Applications) project aims at building an Accelerator Driven System, of which the accelerator will provide a 600 MeV proton beam to a sub-critical nuclear reactor [1, 2]. Apart maintenance interruptions, the nuclear reactor can't stand 10 interruptions longer than 3 seconds per 3-month. The particle accelerator consists of an ion source, a RFQ [3], a normal conducting (NC) linac [4] and a superconducting (SC) linac [5]. The reliability allowing to achieve interruptions of 3 s maximum is based on the components redundancy, so there are two injectors (Fig. 1).
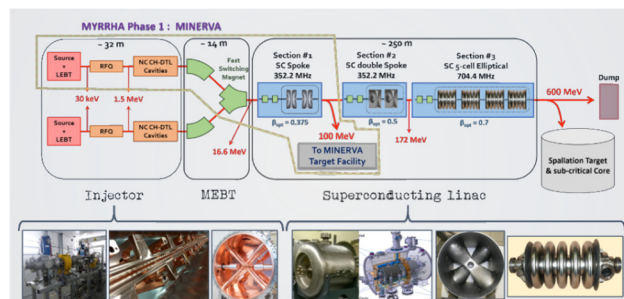

Figure 1: Global MYRRHA accelerator layout.

MINERVA (MYRRHA Isotopes productioN coupling the linEar acceleRator to the Versatile proton target fAcility) is the sub-project of MYRRHA (phase 1) that aims at building the accelerator for physics experiments at 100 MeV [6].

The Deviation Optics

The injectors accelerate the proton beam till 16.6 MeV, hence the protons have a Bρ of 0.6 T.m, which prevents from using electric field. Each injector consists of an ion source, a RFQ, a NC linac and a beam dump. They are parallel and produce a 16.6 MeV proton beam brought to the third part of the medium energy beam transport line (MEBT-3) where the beam dumps and the deviation optics are located. The beam from the first injector is deviated to the SC linac, and in the meantime the beam of the second injector goes straight to a beam dump. The deviation optics of the MEBT-3 selects the beam coming from the injectors with the help of 3 dipole magnets. When a failure occurs in the first injector, the deviation optics of the MEBT 3 switches to the beam of the second injector within 1.5 second.

Among the 3 dipoles, the one situated at the junction of the injection lines (Fig. 2) performs the largest magnetic field flip amplitude from B_0 to $-B_0$, and merges the trajectories of the injectors. The design study of this magnet is presented hereafter.
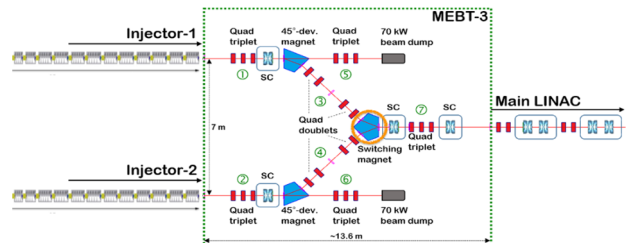

Figure 2: MEBT-3 optics layout with the fast switching magnet in an orange circle.

MAGNETIC DESIGN

Choosing a Structure

The structure of the fast switching magnet was determined mainly by the constraints due to the pulsed magnetic field. Ideally, the inductance (proportional to the pole surface and the relative permeability) should be minimized, to minimize the electric power when the current varies. As the magnet merges the trajectories of the injectors, it has to transport the beam in the same conditions regardless where it comes from.

Following the latter constraint, a round dipole (Fig. 3-1) would have the perfect symmetry to deviate the beam but the reluctance would be high as it is related to the area of the poles and the inverse of permeability.

The second structure in Fig. 3 shows smaller dipoles where the magnetic field would only have to rise from 0 to $|B_0|$, but the space between them makes additional optics

mandatory. This constraint also appears with the third structure (Fig. 3-3), where challenging double aperture quadrupoles (tested on beam transport with field maps in Tracewin [7]) would be necessary in the drift space. So it is not suitable despite it includes the smallest pulsed dipole of the four structures.

The fourth structure considered is compact and tends to minimize the pulsed dipole. It doesn't introduce additional optics, not even pole face angles.
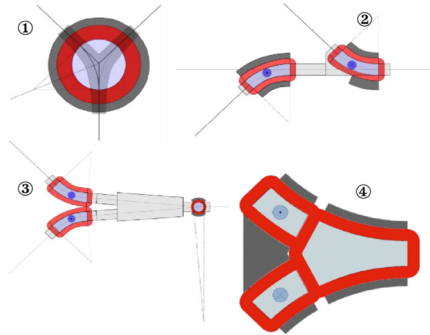

Figure 3: The four structures that can achieve to merge trajectories coming from two directions.

A static and a pulsed dipole form the latter structure. The static dipole generates magnetic fields at B_0 and $-B_0$ in two different gaps, and the pulsed dipole has one pole extending its surface as close as possible to the poles of the static dipole so that the drift space between the dipoles is minimized.

Magnetic Model

At 16.6 MeV, the proton beam $B\rho$ is 0.6 T.m. So to minimize the amplitude of the field flip, the maximum magnetic field is set to 0.5 Tesla leading to a curvature radius of 1200 mm. As the beam diameter is a bit lower than 20 mm at the entrance of the dipole, the gap height is set to 100 mm (Table 1).

Table 1: Geometrical Parameters of the Switching Dipoles

Parameter	Value	Unit
Rms beam diameter	< 20	mm
Nominal field B_0	0.5	Tesla
Curvature radius	1200	mm
Gap height	100	mm
Width of the poles in the static field dipole	158	mm
Shim height	4.5	mm
Static yoke angle	18	degree
Pulsed yoke angle	27	degree
Static current density	8	A/mm^2
Pulsed current density	8.56	A/mm^2
Coils section (w x h)	70 x 38	mm
Yoke material	Low carbon steel	-

The static yoke is a one-piece low carbon steel and the pulsed yoke is laminated (packing factor lower than 1, Fig. 4). The coils have the same section for both dipoles, so the gorges are of same width. 45° chamfers were added to the poles sides to avoid corners saturations. Rounded

shims were added to the poles with a relatively large height due to the width of the poles.
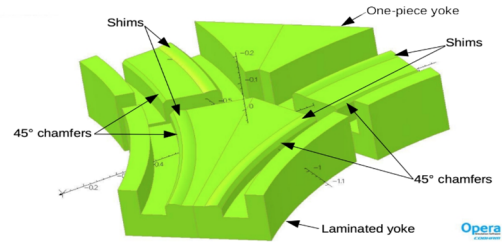

Figure 4: Poles details of both static and pulsed dipoles.

The static poles received a shim only on one side, close to the internal yoke circuit return. The pulsed yoke poles received a shim on both sides.

To avoid loss of magnetic flux, the coils of the pulsed dipole are as close as possible to the surface of the poles. The coils are stacked in the gap between the yokes (Fig. 5), so that the coils of the static dipole are drifted away from the pole surface by the height of the coils.
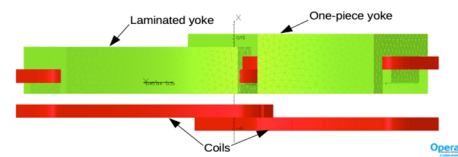

Figure 5: Side view of the dipoles where the stacking of the coils appears in the gap between the yokes.

The OPERA 3D [8] model shows that the pole width, the added chamfers and the shims leave the poles with no saturation (Fig. 6). The small saturation zones at exit corners have no effect on the beam transport simulation with Tracewin.
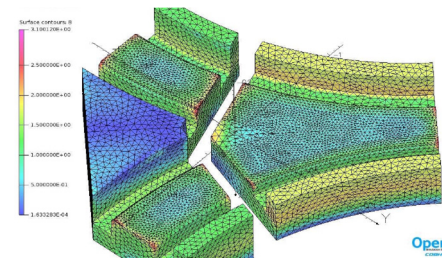

Figure 6: Opera-3D result showing the spread of the magnetic flux on the surface of the yokes.

The Magnetic Field Details

The magnetic field plotted along arcs parallel to the main trajectory in the mid-plane show a decrease of 20% in the gap between the yokes (Fig. 7). As clamping plates were placed at the entrances and the exit, the fringing field has a limited expansion.

On planes away from the mid-plane, field inhomogeneities appear in the static field, whereas inhomogeneities only appear close to the exit of the pulsed dipole (Fig. 8).

Additional beam transport error studies will provide margins for the field homogeneity. At the first try, the deviation performed with such a field map showed an error of only 2 mrad.

MC7: Accelerator Technology
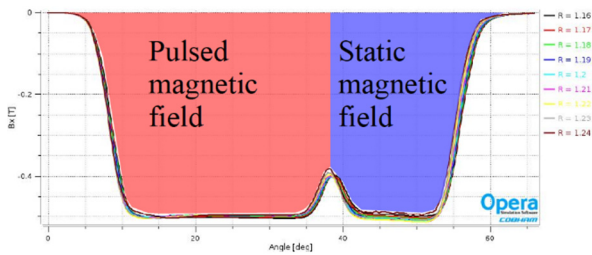
T09 Room Temperature Magnets

Figure 7: Magnetic field plot along arcs parallel to the main trajectory in the mid-plane with radii ranging from 1.16 m to 1.24 m.
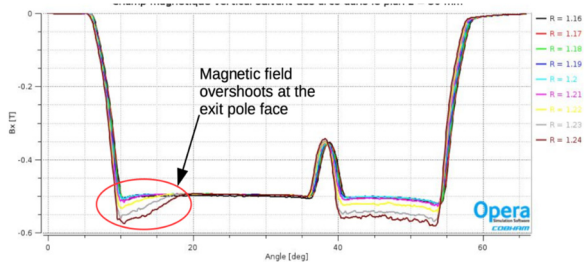

Figure 8: Same arcs as Fig. 7 but at the altitude 30 mm away from the mid-plane, showing the magnetic field inhomogeneities.

The Eddy Currents Effects

The magnetic field should flip from B_0 to $-B_0$ in 1.5 second. The current intensity slope to achieve is then above 1200 A/s. At this rate, eddy currents have strong effects, leading to a delay to reach B_0. The rise time is then the addition of the ramping time and the delay. The simulations, for ramping times of 0.75 s and 1.4 s to increase the field from 0 to B_0 with OPERA3D, showed the delay ranges from 800 ms to 1.05 s depending on the packing factor (Tables 2 and 3).

It proves the need of a regulation system based on the magnetic field measurements as the "b-train" method [9].

Table 2: Eddy Current Delay Measured with OPERA3D

Ramping time 0.75 s				
Packing factor	0.9	0.95	0.971	0.98
B_0 (T)	-0.489	-0.491	-0.492	-0.491
t at 99% of B_0 (s)	1.7	1.7	1.8	1.8
Delay (ms)	950	950	1050	1050

Table 3: Eddy Current Delay Measured with OPERA3D

Ramping time 1.4 s			
Packing factor	0.95	0.971	0.98
B_0 (T)	-0.4910	-0.4908	-0.4915
t at 99% of B_0 (s)	2.2	2.2	2.3
Delay (ms)	800	800	900

MECHANICAL DESIGN

The mechanical design is derived from the OPERA model. The one-piece yoke is made of low carbon steel

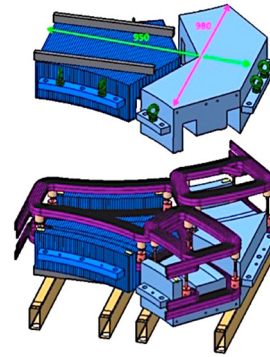XC10 or AISI1010. The pulsed yoke is made of laminations of 0.15 to 0.2 mm thick (Fig. 9).

Figure 9: Exploded view of mechanical design.

The vacuum chamber is unique for the whole dipole structure to avoid mounting operations in the gap between the yokes (Fig. 10). Rectangular section vacuum chambers were studied leading to large defects, so a tubed vacuum chambers was a good compromise for mechanical strength and eddy current minimization.
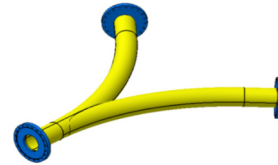

Figure 10: Tubed vacuum chamber of 92.5 mm external diameter and 1.5 mm thick.

The current intensity in the pulsed coils reaches 900 A (Table 4), which implies a water cooling flow rate of 0.5 m^3/h.

Table 4: Current Intensity Parameters in the Pulsed Coils

Parameter	Unit	Value
Current intensity per coil	A	900
Ampère.turns	A.t	21600
Current density	A/mm²	13.3

CONCLUSION

The design proposed allows the beam transport with very small error, so there are no major modifications needed. As already raised, the magnetic field margins (including the size of the "good field region") will be determined by additional beam dynamics error studies using the field maps. As mentioned above, the magnetic field regulation should be studied, specifically using magnetic field measurements to set the slope dB/dt.

The level of mechanical efforts between the static and pulsed dipoles should be calculated to prevent from beam transport perturbations, and provide sufficient mechanical holding.

To estimate the electric power needs, the total inductance of each dipole (static and pulsed) should be calculated.

REFERENCES

[1] The MYRRHA project,
https://myrrha.be/myrrha-project/.

[2] D. Vandeplassche *et al*., "Integrated Prototyping in View of the 100 MeV Linac for Myrrha Phase 1", in *Proc. 9th Int. Particle Accelerator Conf. (IPAC'18)*, Vancouver, Canada, Apr.-May 2018, pp. 661-664.
doi:10.18429/JACoW-IPAC2018-TUPAF003

[3] A. Gatera *et al.*, "Minerva (MYRRHA Phase 1) RFQ Beam Commissioning", presented at the 12th Int. Particle Accelerator Conf. (IPAC'21), Campinas, Brazil, May 2021, paper MOPAB205, this conference.

[4] K. Kümpel *et al*., "Current Status of the MYRRHA Cavities", in *Proc. 10th Int. Particle Accelerator Conf. (IPAC'19)*, Melbourne, Australia, May 2019, pp. 892-894.
doi:10.18429/JACoW-IPAC2019-MOPTS022

[5] F. Bouly, M. Baylac, A. Gatera, and D. Uriot, "Superconducting Linac Design Upgrade in View of the 100 MeV MYRRHA Phase I", in *Proc. 10th Int. Particle Accelerator Conf. (IPAC'19)*, Melbourne, Australia, May 2019, pp. 837-840.
doi:10.18429/JACoW-IPAC2019-MOPTS003

[6] A. Fabich, H. Ait Abderrahim, U. Dorda, and D. Vandeplassche, "Accelerators for Applications in Energy and Nuclear Waste Transmutation", presented at the 11th Int. Particle Accelerator Conf. (IPAC'20), Caen, France, May 2020, paper THVIR15, unpublished.

[7] R. Duperrier, N. Pichoff, and D. Uriot, "CEA Saclay Codes Review for High Intensities Linacs Computations", in *Proc. of the Int. Conf. on Computational Science - Part III (ICCS'02)*, Amsterdam, The Netherlands, Apr. 2002, pp. 411–418. doi:10.1007/3-540-47789-6_43

[8] Dassault Systèmes, SIMULIA Opera-3D,
https://www.3ds.com/products-services/simulia/products/opera/applications/.

[9] H. K. Kuhn and J. D. Pahud, "The Control Systems for the CERN Super Proton Synchrotron Ring Power Supplies", *IEEE Transactions on Nuclear Science*, vol. 28, no. 3, pp. 3102-3104, 1981. doi:10.1109/TNS.1981.4332023